

An unusual case of atypical teratoid/rhabdoid tumor, initially diagnosed as atypical pituitary adenoma in a 13-year-old male patient

Rebecca Ronsley[®], Daniel R. Boué, Lakshmi Prakruthi Rao Venkata, Suzanne Scott, Ammar Shaikhouni, Jeremy Jones, Kathleen M. Schieffer, Catherine E. Cottrell, Elaine R. Mardis, Randal Olshefski, Ralph Salloum and Katherine E. Miller

Division of Oncology, Hematology & BMT, Nationwide Children's Hospital, Columbus, Ohio, USA (R.R., S.S., R.O., R.S.); Department of Pediatrics, The Ohio State University College of Medicine, Columbus, Ohio, USA (R.R., K.M.S., C.E.C., E.R.M., R.O., R.S., K.E.M.); Department of Pathology and Laboratory Medicine, Nationwide Children's Hospital, Columbus, Ohio, USA (D.R.B.); Department of Pathology, The Ohio State University College of Medicine, Columbus, Ohio, USA (D.R.B., K.M.S., C.E.C.); The Steve and Cindy Rasmussen Institute for Genomic Medicine, Abigail Wexner Research Institute at Nationwide Children's Hospital, Columbus, Ohio, USA (L.P.R.V., K.M.S., C.E.C., E.R.M., K.E.M.); Department of Neurosurgery, The Ohio State University College of Medicine, Columbus, Ohio, USA (A.S., E.R.M.); Department of Radiology, The Ohio State University College of Medicine, Columbus, Ohio, USA (J.J.)

Corresponding Author: Katherine Miller, PhD, Institute for Genomic Medicine at Nationwide Children's Hospital, 575 Children's Crossroad, Columbus, OH 43215 (Katherine.Miller@nationwidechildrens.org).

Atypical teratoid/rhabdoid tumor (AT/RT) is one of the most common malignant central nervous system (CNS) tumors in very young children.¹ The hallmark molecular feature of AT/RT is loss of *INI1/SMARCB1* or, less commonly, loss of *Brg1/SMARCA4*.^{2,3} Atypical teratoid/rhabdoid tumor is divided into 3 distinct, core molecular subgroups: AT/RT-SHH, AT/RT-TYR, and AT/RT-MYC.^{4,5} While the typical location of AT/RT in young children is the posterior fossa, in older children, these tumors may occur in other locations, for example, in the pineal or sella/suprasellar region. Furthermore, in addition to diversity in molecular features, each AT/RT subgroup also varies somewhat in terms of age, location, and imaging features.⁴ We describe herein an unusual *SMARCB1*-altered tumor, originally diagnosed as atypical pituitary adenoma (per nomenclature at the time of diagnosis), and ultimately reclassified as Adolescent and Young Adult (AYA)-AT/RT.

Case Description

The patient was a 13-year-old male at the time of diagnosis, who initially presented to a community hospital with headaches and was found to have a mass expanding the sella turcica by head CT and subsequently, an MRI demonstrated a T1 pre- and postenhancing sellar and suprasellar mass with superior displacement of the optic chiasm (Supplemental Figure 1). He underwent resection, and pathology was consistent with atypical pituitary adenoma, with absent immunostaining for thyrotropin/TSH, prolactin, follicle-stimulating hormone, growth hormone, luteinizing hormone, and adrenocorticotrophic

hormone (adequate for classification as “null cell” subtype, at that time in 2010). The tumor was diffusely and strongly pancytokeratin-positive, and patchy-weak synaptophysin-positive with Ki-67 proliferation index over 3%, but still low overall.

During work-up for his suprasellar tumor, he was also found to have panhypopituitarism with gonadotropin, thyroid, and adrenal insufficiency, as well as central diabetes insipidus. In retrospect, the patient endorsed symptoms of pituitary hormone dysfunction for 4 months prior to his brain tumor diagnosis.

Following complaints of increasing headaches, blurred vision, and vomiting, an MRI 2 months postresection revealed tumor recurrence in the left cavernous sinus, and foci of diffusion restriction in the thecal sac suspicious for metastatic disease. The patient underwent additional surgery to biopsy the suspected recurrent metastatic tumor in the left cavernous sinus. Morphology of this sample was identical to that of the prior sample, but the minute tissue quantity, and crush artifact, at that time limited further studies; however, based on testing completed and multidisciplinary review, the pathological diagnosis was deemed consistent with pituitary carcinoma, given metastatic dissemination. Cerebrospinal fluid (CSF) staging evaluation was negative. He was started on temozolomide in tandem with craniospinal radiation.

Six months after completion of maintenance chemotherapy, there was a radiologic concern for recurrent tumor in the left cavernous sinus for which he underwent Gamma knife treatment. The patient again experienced recurrent tumor growth 2 years after Gamma knife, for which he was treated with temozolomide but was only able to tolerate for 3 months. On surveillance MRI, performed 10 years after initial presentation

at age 23, a soft tissue mass within Meckel's cave was detected and resected. Given this new, late tumor presumed to be a recurrence, the original primary tumor tissue was obtained from pathology archives for re-evaluation, warranted by the availability of newer diagnostic techniques including immunohistochemical stains not available at the time of original diagnosis.

This case was reviewed by a multidisciplinary team including members of neuro-oncology, neurosurgery, radiology, neuropathology, and genomics. The patient also consented to a translational research protocol which included exome sequencing of both the original primary tumor and this new presumed recurrence, nondisease-involved brain tissue, and buccal tissue, plus DNA array-based methylation profiling of both tumors. Exome sequencing of DNA derived from the buccal epithelium (serving as a comparator) and brain tissues was performed using NEBNext Ultra II FS DNA kit with paired-end Illumina sequencing to achieve >200x depth (see [Supplementary Material](#) for more details). Routine H&E-stained sections of

the recurrent/secondary tumor showed pattern-less sheets of relatively monotonous epithelioid tumor cells, with generally round to ovoid nuclei, often distinct nucleoli, and a moderate volume of monomorphic cytoplasm, without any obvious, conspicuous, or definite rhabdoid-like cytoplasmic inclusions ([Figure 1A](#)). Immunohistochemistry (IHC) for Ki-67 showed a relatively low tumor nuclear proliferation index overall ([Figure 1B](#)). Immunohistochemistry for Pan-Cytokeratin showed diffusely strong staining/expression in tumor cell cytoplasm. ([Figure 1C](#)). The tumor cells were clearly INI-1 negative ([Figure 1D](#)). The newly detected tumor and the original primary tumor were thus reclassified and classified as AT/RT, as indicated by the morphology and near-total loss of INI-1 expression in tumor nuclei. Based on tumor reclassification as AT/RT, the patient underwent focal radiation therapy and was initiated on chemotherapy as per the Children's Oncology Group protocol, ACNS0332.

Exome sequencing revealed that the *SMARCB1* variant was enriched in both the primary and secondary tumor

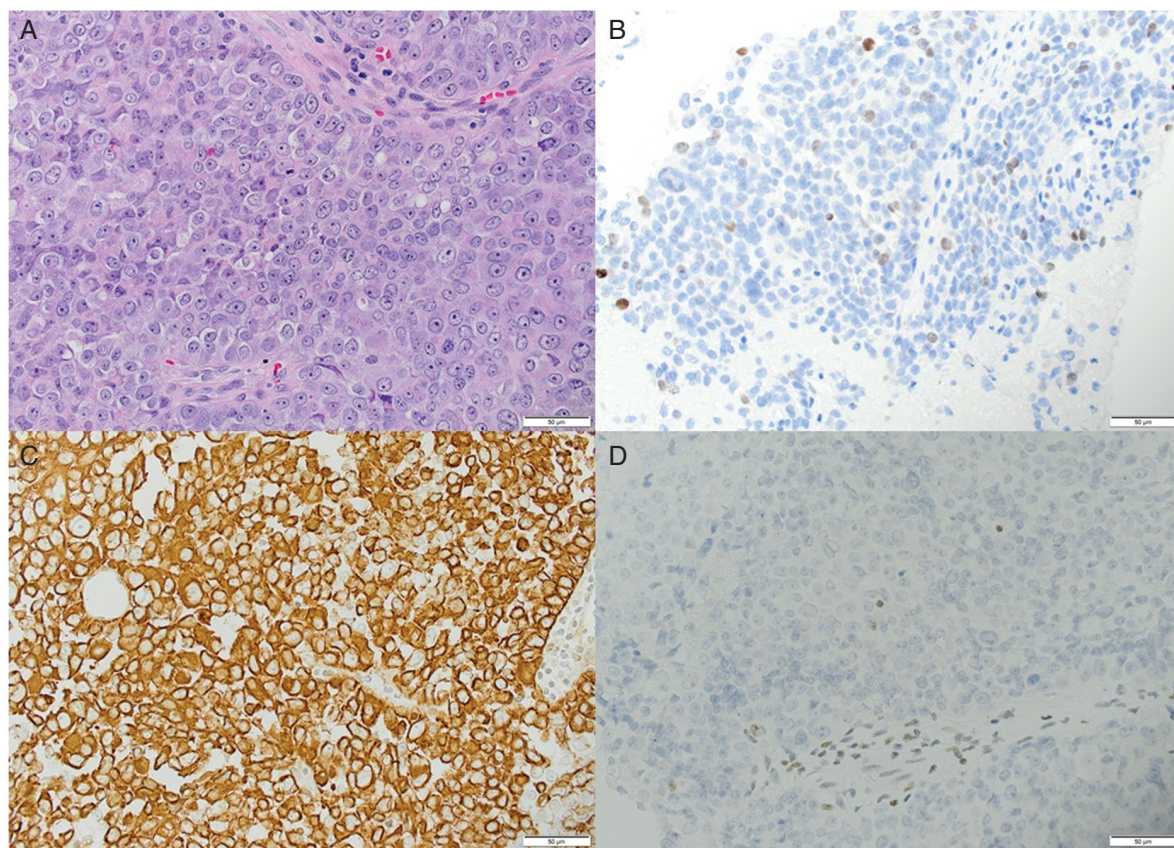


Figure 1. Histopathological features of the primary tumor. (A) The 2010 (original primary AYA AT/RT) routine H&E-stained section showing epithelioid tumor cells, with generally round to ovoid nuclei, often distinct nucleoli, and a moderate volume of monomorphic cytoplasm, without any obvious or conspicuous rhabdoid-like cytoplasmic inclusions, at 40x objective magnification. (B) The 2010 (original primary AYA AT/RT) tumor with IHC for Ki-67, showing a relatively low tumor nuclear proliferation index, at 40x objective magnification. (C) The 2010 (original primary AYA AT/RT) tumor with IHC for pan-cytokeratin, showing diffusely strong staining/ expression in tumor cell cytoplasm, at 40x objective magnification. (D) The 2010 (original primary AYA AT/RT) tumor with IHC for INI-1, showing near-total loss of staining/ expression in tumor cell nuclei, but retained expression in normal vascular endothelial (lower 1/2) and scattered inflammatory cell nuclei, at 40x objective magnification.

tissues at 54% and 33% variant allele frequency (VAF), respectively (Figure 2A). Exome-based copy number plots indicated both primary and secondary tumors exhibited copy neutral loss of heterozygosity (LOH) of 22q, a region which includes the *SMARCB1* gene, consistent with the observed increase in VAF with loss of the second allele constituting the second hit in the tumor (Figure 2B). No other pathogenic variants were identified in the tumor samples. Exome sequencing revealed a pathogenic *SMARCB1* variant (NM_001362877.2: c.825_826dup; p.Ser258Cysfs*10) that was suspected to be somatic mosaic as the VAF was only 19% in buccal tissue. Additional sequencing in nondisease-involved brain tissue confirmed the *SMARCB1* variant to be of somatic mosaic etiology at 11% VAF, thus this individual demonstrates mosaicism in association with Rhabdoid Tumor Predisposition Syndrome (RTPS) caused by postzygotic variation during development. The patient and his family underwent genetic counseling; however, given his age being outside of the published surveillance

recommendations for SMARCB1 mutations, no screening was recommended.

DNA array-based methylation profiling using the DKFZ DNA methylation brain tumor classifier version v11b6⁶ displayed the highest scoring classification of each tumor in association with the AT/RT family (albeit at diminished confidence <0.9), with the primary tumor classifying most closely as class: AT/RT-TYR (0.3642), and the new tumor displaying the highest AT/RT class in association with, AT/RT-MYC (0.2294) (Table 1).⁷ Using the more recently updated classifier v12.5, the tumor methylation data were reanalyzed, and the original primary tumor was again classified as AT/RT (score 0.8732) with a TYR subgroup classification (score 0.3607). The highest subgroup classification in the newly detected tumor was associated with AT/RT-MYC (score 0.1129). Clustering by UMAP analysis, using AT/RT samples from our institution and from the DKFZ database, demonstrated that the primary tumor clustered most closely with other AT/RT-TYR samples, while the recurrent/

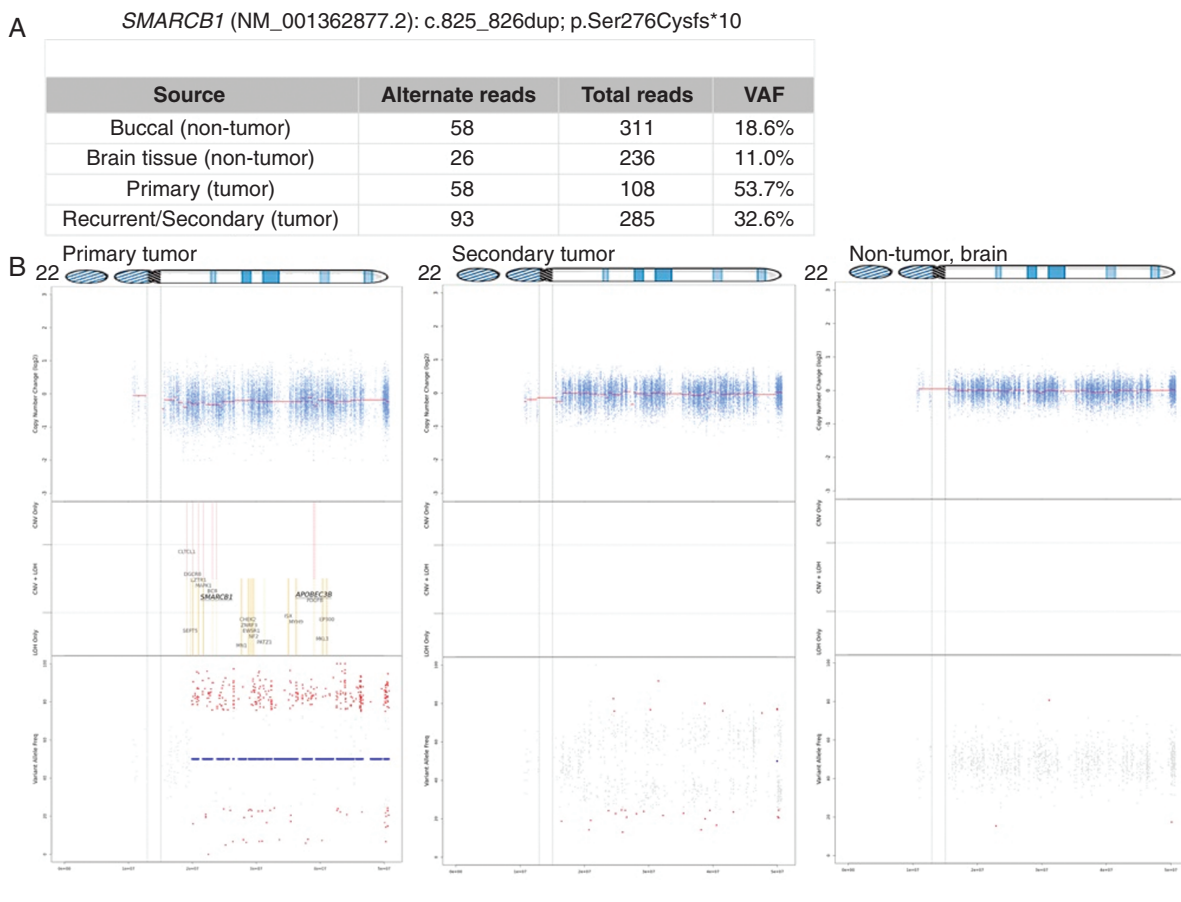


Figure 2. *SMARCB1* alterations in patient tumor and comparator tissue. (A) A 2-bp duplication was identified in all specimens studied, and total sequencing read depth and corresponding variant allele frequencies (VAF) for each tissue are shown. (B) Genome-wide copy number plots for chromosome 22 for primary (left) and secondary tumor (middle) and non-tumor adjacent brain (right) are shown; on the top window of each panel are copy number plots, where the dots represent the log₂ copy number ratio for the tumor relative to the normal specimen and the horizontal lines represent CNV segments; the heterozygosity plots (bottom window of each panel) show the tumor VAF for heterozygous germline variants; the middle window of each plot shows the label of any cancer genes that fall within the CNV-affected regions.

Table 1. Methylation profiling of primary and secondary tumor

	Primary Tumor	Secondary Tumor
Sample type	FFPE	Frozen
Tumor purity (ESTIMATE)*	87.9%	67.9%
Tumor purity (pathology)**	90%	10%
DIN***	5.5	7.4
Methylation (classifier v11b6)	Family: AT/RT (0.7758) Class: AT/RT-TYR (0.3642)	Family: AT/RT (0.3185) Class: AT/RT-MYC (0.2294)
Methylation (classifier v12.5)	AT/RT (0.8732) AT/RT-TYR (0.3607)	AT/RT-MYC (0.1129)

Methylation classifier scores are listed in parentheses.

*Tumor purity predicted by ESTIMATE using RNA-sequencing gene expression data.⁷

**Tumor purity estimated by pathologist.

***DIN (DNA Integrity Number) predicted using Agilent 2200 TapeStation system

Abbreviations: AT/RT, atypical teratoid rhabdoid tumor; FFPE, formalin-fixed paraffin-embedded; MYC, myc subtype of AT/RT; TYR, tyrosinase subtype of AT/RT

secondary tumor did not clearly cluster tightly with any specific subgroup (Supplemental Figure 2). Furthermore, RNA-seq data from this patient plus 6 other AT/RT samples from our institution were used to interrogate expression of subgroup-specific marker genes for MYC (*MYC & HOTAIR*), SHH (*MYCN & ASCL1*), and TYR (*TYR & MITF*) subgroups. Both primary and secondary tumors had expression of MYC (but not *HOTAIR*), and neither tumor had high expression of SHH or TYR subgroup marker genes (Supplemental Figure 3), reinforcing the unusual nature of this tumor.

By histopathology, the secondary/recurrent tumor was suggested to most likely represent (and was morphologically and immuno-phenotypically consistent with) a late recurrent AT/RT; however, given the patient's somatic mosaic *SMARCB1* alteration associated with RTPS and the fact that the secondary/recurrent tumor was not in the same precise location as the original primary tumor of the sella turcica, it was considered that this new presumed recurrent tumor could potentially represent, instead, a later onset new primary AT/RT. Additional evidence for this latter possibility was some variation in IHC-staining patterns seen when comparing the original primary and presumed recurrent tumors. The secondary/recurrent tumor was less pan-cytokeratin-positive, far more strongly synaptophysin-positive, and showed a significantly higher Ki-67 proliferation index at about 25% positive regionally, compared to a much lower Ki-67 index ($\leq 10\%$) in the original primary tumor. Such differences could perhaps also result from clonal evolution. Following re-resection, the patient went on to receive 6 cycles of maintenance chemotherapy with cyclophosphamide and vincristine. Cisplatin was omitted due to patient's high-frequency sensorineural hearing loss. End-of-therapy MRI revealed no evidence of tumor recurrence.

Discussion

Atypical teratoid/rhabdoid tumor is a relatively rare tumor that typically occurs in young children (usually

<6 years old). Herein, we present an AYA patient whose sellar region tumor was initially diagnosed as an atypical pituitary adenoma and subsequently reclassified as AT/RT, utilizing both histopathological re-evaluation and updated testing, and DNA methylation analysis. In this case, the newer/more recent literature, well describing the AYA-ATRT entity prompted the neuropathologist to perform an INI-1 stain on the original sample from 2010. This led to further testing and ultimately the patient's molecularly confirmed diagnosis. As our understanding of these rare tumors expands, this case highlights the importance of reconsidering one's differential diagnoses in tumors like this one.

The clinical differential diagnosis of the original tumor was adenoma versus low-grade glioma versus germ cell tumor versus embryonal tumor; however, given the radiographic features and the morphology, consensus at that time was that this was most consistent with adenoma. The histopathological differential diagnosis for the original tumor also favored pituitary adenoma. The original differential was more extensive, but with IHC-staining patterns essentially excluding the following 4 other main diagnostic considerations: germ cell tumors (AFP, HCG, CD30, CD117, OCT4, SALL4, and PLAP—all negative); parameningeal rhabdomyosarcoma (myogenin, MyoD1—both negative); melanoma (HMB45—negative); unusual glioma (S100, GFAP—both negative). Meanwhile, the weak synaptophysin reactivity, strong pan-cytokeratin staining, somewhat increased Ki-67 and p53 staining for typical adenoma, all seemingly aligned best (at the time) with a presumed null cell subtype "atypical" adenoma, which was supported by imaging, location, patient age, morphology, and relatively low Ki-67 index.

Interestingly, on an initial review of the original tumor's histomorphology and IHC-staining profile, this neoplasm seemed to align well with an atypical null cell adenoma (as was defined in 2010). In 2010, IHC staining for INI-1 was not widely available. Second, the tumor was both strongly pan-cytokeratin-positive, and patchy/weakly positive for synaptophysin, typical and nearly diagnostic of null cell adenoma. It should be noted that following the time of this

patient's original diagnosis, it has become well known that AT/RT is frequently poly-phenotypic in this way. Further, the sellar location, the AYA patient age (13 years old at the time of original diagnosis), the lack of clear rhabdoid inclusions, and the low Ki-67 proliferation index, all pointed toward adenoma and away from AT/RT at that time.

As molecular testing becomes more advanced and more widely available, it is not uncommon for tumors to be reclassified, including as AT/RT, after an initially different diagnosis. In fact, one recently published case of AT/RT was in an adult female previously diagnosed with a lactotroph adenoma.⁸ As with our patient, that tumor was also located in the sellar region.

Although many features of this neoplasm are consistent with what is more currently described for AT/RT, there are several unique features. Our patient was a 13-year-old male at original diagnosis, much older than the typical pediatric AT/RT patient. In adults, AT/RT cases predominantly occur in the sellar region or superficial cortex,^{4,9} which is consistent with our patient's tumor. However, nearly all prior AYA or adult patients with sellar region AT/RT described in the literature to date occur in females, and our patient is male. In one review of patients of all ages with sellar AT/RT, all 18 identified patients were female.⁹

Overall, the histopathological and immunophenotypic features of this tumor were consistent with AT/RT; however, on review of prior reported cases of AYA AT/RT, these are much more frequently CD34-positive than AT/RT in younger patients.^{10,11} This patient's tumor was entirely CD34-negative, both the original primary and the new presumed recurrence. Also, the Ki-67 proliferative index (<10%+) at original diagnosis does not align well with the usual pediatric AT/RT; however, more recent literature has suggested that such low Ki-67 proliferative indices may be seen in some AYA AT/RT.¹¹

The molecular features of this case are consistent with AT/RT, especially given the *SMARCB1* pathogenic alteration, which predisposes to the development of rhabdoid tumors. Further, the methylation arrays performed on the original primary tumor support the diagnosis of AT/RT, using the v11b6 version of the DKFZ brain tumor classifier; the lower score for the new tumor may be due to lower estimated tumor content of 68%. Also of note, previously published cases of AT/RT in older patients are most commonly AT/RT-MYC subgroup,⁴ whereas in this case, the initial tumor classified as AT/RT-TYR subgroup. Using an updated version v12.5 of the DKFZ brain tumor classifier, the primary tumor confidently matched with AT/RT (score 0.8732) in the TYR subgroup (score 0.3607), while the secondary tumor matched in the MYC subgroup (score 0.1129). It cannot be concluded that this AT/RT definitively experienced subgroup switching (from TYR to MYC) given the low confidence scores for the methylation subgroup classifications. Rather, the lower subclassification scores are likely attributed to the uniqueness of this tumor we describe, whereas AT/RT in the reference cohort of the DKFZ brain tumor classifier likely represents more "typical" AT/RT in terms of patient age, tumor location, and histopathology. As well, in prior reports, the described cases were in older adults, again differing from our case, an AYA patient.

This case represents an unusual *SMARCB1*-altered tumor of the sella that was originally diagnosed as atypical pituitary adenoma, but subsequently reclassified as AT/RT following extensive histopathological re-evaluation, molecular analysis of archival original primary and the presumed recurrent tumor. This young adult male is currently disease-free following multimodal therapy. Genomic profiling enabled diagnosis with mosaic RTPS, and this individual has received appropriate surveillance and counseling for future reproductive risk. This report emphasizes the role of molecular testing in making the correct diagnosis for this unusual tumor and highlights the clinical-pathologic and molecular heterogeneity of this tumor.

Supplementary material

Supplementary material is available at *Neuro-Oncology Advances* online.

Keywords

adolescents and young adults (AYA) cancer | atypical teratoid rhabdoid tumor (AT/RT) | central nervous system (CNS) tumor | DNA array-based methylation profiling | pediatric cancer

Funding

Molecular analyses were supported by the Nationwide Foundation Pediatric Innovation Fund.

Conflict of interest statement. The authors declare that they have no competing interests.

Authorship statement

Formal analysis: RR, DRB, LPRV, KMS, RS, KEM; Investigation: DRB, LPRV, KEM; Resources: RR, DRB, JJ, SS; Writing- Original Draft: RR, DRB, KEM; Writing- Review & Editing: All authors; Supervision: CEC, ERM, RO, RS

Ethics approval and consent to participate

Written informed consent was obtained for this study under a research protocol approved by the Institutional Review Board at Nationwide Children's Hospital (IRB17-00206).

Availability of data and material

DNA exome sequencing data for this study has been deposited to dbGaP under accession number phs001820.v1.p1. Identifiers are: IGMCH0084_S-2021-006926 (buccal tissue), IGMCH0084_S-2021-012939 (brain, adjacent normal), IGMCH0084_S-2021-006933 (primary brain tumor), and IGMCH0084_S-2021-012111 (recurrent brain tumor).

References

1. Fruhwald MC, Biegel JA, Bourdeaut F, Roberts CW, Chi SN. Atypical teratoid/rhabdoid tumors-current concepts, advances in biology, and potential future therapies. *Neuro-Oncology* 2016;18(6):764–778.
2. Hasselblatt M, Isken S, Linge A, et al. High-resolution genomic analysis suggests the absence of recurrent genomic alterations other than SMARCB1 aberrations in atypical teratoid/rhabdoid tumors. *Genes Chromosomes Cancer* 2013;52(2):185–190.
3. Hasselblatt M, Nagel I, Oyen F, et al. SMARCA4-mutated atypical teratoid/rhabdoid tumors are associated with inherited germline alterations and poor prognosis. *Acta Neuropathol.* 2014;128(3):453–456.
4. Johann PD, Bens S, Oyen F, et al. Sellar region atypical teratoid/rhabdoid tumors (ATRT) in adults display DNA methylation profiles of the ATRT-MYC subgroup. *Am J Surg Pathol.* 2018;42(4):506–511.
5. Johann PD, Erkek S, Zapatka M, et al. Atypical teratoid/rhabdoid tumors are comprised of three epigenetic subgroups with distinct enhancer landscapes. *Cancer Cell.* 2016;29(3):379–393.
6. Capper D, Jones DTW, Sill M, et al. DNA methylation-based classification of central nervous system tumours. *Nature* 2018;555(7697):469–474.
7. Yoshihara K, Shahmoradgoli M, Martínez E, et al. Inferring tumour purity and stromal and immune cell admixture from expression data. *Nat Commun.* 2013;4:2612.
8. Barresi V, Lioni S, Raso A, et al. Pituitary atypical teratoid rhabdoid tumor in a patient with prolactinoma: a unique description. *Neuropathology* 2018;38(3):260–267.
9. Nakata S, Nobusawa S, Hirose T, et al. Sellar atypical teratoid/rhabdoid tumor (AT/RT): a clinicopathologically and genetically distinct variant of AT/RT. *Am J Surg Pathol.* 2017;41(7):932–940.
10. Chan V, Marro A, Findlay JM, Schmitt LM, Das S. A systematic review of atypical teratoid rhabdoid tumor in adults. *Front Oncol.* 2018;8:567. eCollection 2018.
11. Bodi I, Giamouriadis A, Sibtain N, et al. Primary intracerebral INI1-deficient rhabdoid tumor with CD34 immunopositivity in a young adult. *Surg Neurol Int.* 2018;9:45. eCollection 2018.